

Variations in short-term statistics of waves observed in the coastal waters of the eastern Arabian Sea

Anusree A, V Sanil Kumar*

Ocean Engineering, CSIR-National Institute of Oceanography
(Council of Scientific & Industrial Research),
Dona Paula, Goa - 403 004 India

*Corresponding author Tel: 0091 832 2450 327 email: sanil@nio.org

Abstract

Understanding the short-term statistics of waves is crucial for various marine applications. Present study investigates variations in the short-term statistics of waves in the eastern Arabian Sea, at a water depth of 15 m utilizing 172,704 30-min-long sea state records from 2010 to 2020. The maximum recorded individual wave height during the study period is 8.3 m. Individual wave period, height, length and steepness are higher during the monsoon (June-August). Consequently, the number of waves is lower than it is in the non-monsoon. Moreover, there are high energy swells during high wave events, and during the non-monsoon, the wave spectrum is multi-peaked, with low-frequency swells and high-frequency wind-seas. The crest height of the largest wave in different years during the study period is 0.57-0.60 times the wave height. The characteristic wave height, $H_{1/10}$, is 1.24 times the significant wave height, and the maximum wave height is 1.6 times the significant wave height. Significant inter-annual variability exists in the exceedance probabilities of waves with higher heights. For the extreme sea state, the probability of the exceedance of normalized wave heights is in good agreement with the Rayleigh, Forristall and Van Vledder distributions. However, the crest heights only follow the Rayleigh distribution.

Keywords: Surface waves, maximum wave height, zero-up-crossing analysis, wave height distributions

1. Introduction

The wind waves or ocean surface waves generated by winds blowing over the ocean surface are random in nature and are a key factor in planning marine operations and air-sea interaction studies (Kinsman, 1965). The wave field at most locations represents the wind-seas (locally forced waves) superimposed on the swells (remotely forced waves) (Sverdrup and Munk, 1947). Waves have a range of wave periods (T) and are associated with a range of heights (H). A sea state is defined as a duration in which the wave conditions can be considered almost stationary, with the period normally defined in the range of 0.5 to 3 h, and it is represented in terms of significant wave height ($H_{1/3}$ or H_s) and mean wave period ($T_{1/3}$ or T_{m02}). Characteristic wave parameters like significant wave height, mean wave period and mean wave direction are used for specifying the wave conditions.

Identifying the wave height distribution is crucial for determining wave heights with different exceedance probabilities. Quantifying the probability of a wave height exceeding a critical height is an essential step in designing marine structures and vessels, and it is also used in the evaluation of high wave height. Numerous studies have explored the importance of wave height distributions (e.g., Goda, 2010; Guedes Soares, 2003; and the references therein). Moreover, information on the characteristics of high waves is necessary for marine operations and the design of coastal and offshore facilities. Different methods have been used to predict the probabilistic nature of sea waves. Based on the linear model of waves with a narrow energy spectrum, it is shown that the short-term statistics of wave heights in deep water (see Ochi, 1998, for a review) follow the Rayleigh distribution (Longuet-Higgins, 1952). Longuet-Higgins (1952) introduced the Rayleigh distribution based on the assumptions of a stationary Gaussian ocean surface and a narrow spectrum, in which the parameter of the distribution is $a=H_{rms}$. When time series is not available but only spectral data is, $a=\sqrt{8m_0}$ can be used, and the distribution is then known as the spectral Rayleigh distribution. According to Forristall (1978), the Rayleigh distribution overpredicts the probabilities of the highest waves. Forristall analysed 116 hours of hurricane-generated waves in the Gulf of Mexico and the data were empirically fitting to a Weibull distribution and suggested a two-parameter Weibull distribution as in Appendix-I. Dattatri et al. (1979) examined the distribution of height and period of waves recorded off Mangalore, the west coast of India. The observed statistics of extreme waves deviate from the values based on the Rayleigh distribution (Stansell, 2004; Mori and Janssen, 2006). Casas-Prat and Holthuijsen (2010) examined the height distributions of 10,000,000 deep water waves obtained from buoy measurements in the Mediterranean Sea off the coast of Spain. Amrutha and Kumar (2015) reported that the significant wave height is ~8% lower than that projected by the

Rayleigh distribution for waves measured at a water depth of 13 m. Measurements of individual wave heights and crest heights at 190 m water depth in the northern North Sea show that for individual wave height and crest heights in long-crested seas, Forristall distribution is considered to provide the most appropriate descriptions of these measured wave data (Kvingedal et al., 2018). Orimoloye et al. (2019) observed that the Rayleigh distribution could not properly represent bimodal seas with wider spectral widths. Furthermore, Karpadakis et al. (2020) explained that different distribution models perform depending on relative depth, spectral bandwidth and steepness based on the data from the central and southern North Sea. The investigation of short-term statistics of waves with significant wave heights greater than 3 m in coastal waters around the United Kingdom (over 40,000 half-hour-long records) indicate that the Rayleigh distribution with parameter $a = H_{rms}$ has lower errors than other models in the estimation of $H_{1/3}$ (James and Panchang, 2022).

The design criteria for coastal facilities require characteristic wave heights such as $H_{1/3}$ (the average of the highest one-third of all wave heights) or $H_{1/10}$, which is a wave height with an exceedance probability of 10% (the average of the highest one-tenth of all wave heights). If the wave heights follow the Rayleigh distribution, these characteristic heights can be converted into another through known constants. When designing the deck elevation of an offshore platform, the crest height of the wave is more of interest than the total wave height (Goda, 2010). For ship routing and ship design, European regulations define ship design standards in relation to $H_{1/10}$. In marine engineering applications, larger wave heights (H_{max} and $H_{1/10}$) are essential, but they may not be readily available (Nayak and Panchang, 2015). Hence, it is important to know the variations of different wave parameters at a location.

The wave period corresponding to a particular wave height is essential for various marine operations and construction projects. The early studies done by Battjes (1970) gave the joint distribution of $H_{1/3}$ and the mean wave period. The probability-based design of offshore structures generally requires $H_{1/3}$ and the mean wave period to describe the long-term wave climate (Mathisen and Bitner-Gregersen, 1990) from the respective distribution of individual wave heights. Hence, it is of prime importance to find a wave period associated with a wave height.

Wave steepness (wave height/wave length) is a measure of wave stability, with steeper waves causing a greater hazard. As the waves approach the nearshore, wave height increases, wavelength decreases and steepness increases. In coastal regions, smaller vessels may capsize when the steepness increases. Hence, it is essential to determine the steepness of waves in coastal waters, especially when the wave heights are large.

The eastern Arabian Sea is exposed to swells from the Southern Ocean and the south Indian Ocean. Hence, the waves will be swells superimposed on wind-seas (Dora and Kumar, 2015). During the monsoon period (June-August), the coastal waters of the eastern Arabian Sea experience a rough sea state ($H_{1/3} > 1.5$ m). Since the Arabian Sea is characterised by strong seasonality due to change in the direction of the monsoonal wind (Schott and McCreary, 2001), significant changes in wave characteristics are observed with the seasons. Hence, it is necessary to examine the monthly variations in wave parameters.

Considering the above, the present study assesses the monthly and inter-annual variability in the short-term statistics of waves in coastal waters. The main objective of the analysis is to identify a distribution function for individual wave height and crest height. The rest of the paper is arranged as follows. Section 2 presents a description of the data used and the methodology, and Section 3 compares the main wave parameters along with the results and discussions. The summary and conclusions are presented in Section 4.

2. Data and methods

The wave data used for this study were measured off Karwar, located in the eastern Arabian Sea at 15 m water depth (14.822° N; 74.052° E). The data were collected using a moored Datawell MKIII directional waverider buoy from 1 January 2010 to 31 December 2020. The waverider buoy recorded the two horizontal (north-south and east-west) and vertical accelerations of the buoy, and the corresponding translational motions were estimated (Datawell, 2009).

Vertical displacement is measured with 1 cm resolution and 3% accuracy. The height (H) and period (T) of the individual waves are obtained following the zero-up-crossing method (Tucker, 1991). $H_{1/3}$, $H_{1/10}$ and the significant wave period ($T_{1/3}$) are obtained from individual waves in a 30-min sampling period. The crest height (H_c) and trough depth (H_t) are calculated from heave data. The maximum height of the wave in a 30-min record is the maximum wave height (H_{max}). Wave length (L) at the measurement location is computed from the wave period and the water depth (d) by solving the wave dispersion relation iteratively.

The wave spectrum of surface elevation is computed from the heave data measured for 30 min through the Fast Fourier Transform (FFT). The wave spectrum has a resolution of 0.005 Hz from 0.025 Hz to 0.1 Hz and 0.01 Hz from 0.1 Hz to 0.58 Hz (Datawell, 2009). Spectral moments (m_n) and the spectral peak period (T_p) are derived from the wave spectrum. The significant wave height (H_{m0}), energy wave period ($T_{m-1,0}$) and average wave period ($T_{m-1,1}$) are computed from the spectral moments. The n^{th} order spectral moment is obtained as $m_n = \int_0^{\infty} f^n S(f)df$, where $S(f)$ is the

spectral energy density at frequency f . The spectral narrowness parameter (ν) (Longuet-Higgins, 1975) and spectral width parameter (ε) is used as an indicator of the strength of non-linear focusing and estimated using equation (1). Both ν and ε vary from 0 to 1 with lower values for the narrow-band spectrum, i.e., the energy is concentrated near the spectral peak frequency, as individual waves have similar frequencies with differing amplitudes. The other parameter evaluated to examine the peakedness of the wave spectrum is the spectral peakedness parameter (Q_p) (Goda, 1970). The value of Q_p is infinite for a single frequency wave spectrum i.e., extremely narrow-banded, and is unity for an extremely broad-banded. The skewness and kurtosis of the free surface elevation are computed to study the non-linearity of the wave fields. The directional width or the spread parameter is estimated following Kuik et al. (1998).

$$\text{Spectral narrowness parameter } (\nu) = \sqrt{\frac{m_2 m_0 - m_1^2}{m_1^2}} \quad (1)$$

$$\text{Spectral width parameter } (\varepsilon) = \sqrt{\frac{m_0 m_4 - m_2^2}{m_0 m_4}} \quad (2)$$

The annual probability of the exceedance of observed characteristic wave heights ($H_{1/3}$, $H_{1/10}$ and H_{\max}) and corresponding wave periods ($T_{1/3}$, $T_{1/10}$ and $T_{H_{\max}}$) are compared for the years with more than 95% data. The years with fewer data are not considered for comparison since the behaviour of the distribution changes with data less than 95%. The six selected years are 2011, 2012, 2014, 2016, 2017 and 2018. The probability of exceedance of the wave heights and crest heights of each 30-min record is calculated and compared with six selected wave height distribution models. The wave height distribution models (James and Panchang, 2022) examined in the study are presented in Appendix-1. The number of sea states falling in each bin is counted. To calculate the probability of the exceedance of the observed wave heights and periods, 0.2 m bins (i.e., 0.0-0.2 m, 0.2-0.4 m ...) and 1 s bins (i.e., 0-1 s, 1-2 s ...) are considered, respectively. In order to estimate the probability of exceedance of a certain wave height, the ratio between the sum of the number of data in the consecutive bins up to the selected height and the total number of data in that particular period of the analysis is calculated. The exceedance probability is estimated by subtracting this ratio from 1 (WMO, 1998). The observed probabilities for a sea state are compared with model values using bias, which is calculated as the mean of differences between the observed and the model values.

3. Results and discussions

3.1 Wave characteristics

Observed half-hour-long sea state records at a 15 m water depth off Karwar from 2010 to 2020 have been analysed. Even though the data were collected continuously, there are data gaps in some years due to the drifting of the buoy from its deployed location (resulting from accidental entanglement with fishing nets) and the retrieval of the buoy for routine maintenance. A total of 172,704 half-hour data sets are used in the study (Table 1). The percentage of data recorded, the total number of waves, and the number of sea states with $H_{1/3}$ less than or equal to 1.5 m, $H_{1/3}$ between 1.5 m and 3 m, and $H_{1/3}$ greater than or equal to 3 m in each year is presented in Table 1. The number of data is fewer in 2010, out of which 95.14% have a significant wave height ($H_{1/3}$) less than or equal to 1.5 m and only three datasets have a significant wave height greater than or equal to 3 m. Of the years in the study period, 2011 has the maximum number of data (17,517). The number of sea states with $H_{1/3}$ equal to or greater than 3 m is the highest (415) in 2018. Over the period of one year, 5,395,125 to 5,534,980 waves were measured in different years and the average height and period of these waves were 0.65 m and 5.7 s (Table 1). A total of 32,843,173 waves were measured during 2011, 2012, 2014, 2016, 2017 and 2018. The annual maximum wave height ranged from 4.8 m in 2010 to 8.3 m in 2020. The largest wave period is 22 s, the maximum observed $H_{1/3}$ is 4.8 m, and the maximum wave height is 8.3 m. The sea state containing the high waves that are measured has a significant wave height ($H_{1/3}$) of 2.6-4.3 m and a peak period T_p of 10.5-13.3 s, and those waves are from 238 to 263°.

The heights of individual waves show a seasonal variation and are higher (with a monthly average value of 1.2-1.4 m) from June to August (the monsoon period), and they are lower (0.3-0.35) from November to February (Fig. 1b). The number of waves is less from June to September, whereas a large number of waves (555,226-567,719) are observed in January (Fig. 1a), since the mean wave period is low in January. The individual wave period (Fig. 1c) and wave length (Fig. 1d) in October 2016 is slightly less than the rest, whereas it is higher in November. The steepness of individual waves is not more than 0.028, with the minimum occurring during October-March. The monthly average value of wave length ranges from 36 to 67 m, but the maximum wave length is 267 m. For the data analysed, the d/L values range between 0.051 and 3.751 and the monthly average values range from 0.42 to 0.79 with an average of 0.62, indicating that all the waves measured are intermediate or deep-water waves (Fig. 1f). Note that the d/L value is low from June to August, since the wave period increases with an increase in height due to the monsoon.

In a year, the largest wave heights generally occur either in June or July. However, in 2011, 2019 and 2020, the highest waves occurred in September, October and August, respectively (Table 2). In 2019, the annual maximum significant wave height of 5.1 m occurred in October for the first time in the last 42 years at the study location due to the impact of the tropical cyclone Kyarr (Nair et al., 2022). The length of the largest wave varies from 96 to 139 m in different years (Table 2), while the steepness ranges from 0.035 to 0.080 and is smaller than the steepness of the wave-breaking limit ($\sim 0.142 \tanh(kd)$, where k is the wave number and d is the depth).

3.2 Relation between characteristic wave heights and periods

To gain an idea of how wave heights change with corresponding wave periods, a scatter diagram has been plotted between periods and the square root of heights. The analysis is done for 2011 since that year has 99.98% of the data. Earlier studies suggest that the best-fit slope for the plot between peak wave periods and the square root of heights ranges from 2.6 to 3.9 (ISSC, 1979). For the original JONSWAP spectrum, the slope value is ~ 4.5 . However, the present data between $T_{1/3}$ and $H_{1/3}$, $T_{1/10}$ and $H_{1/10}$ and $T_{H_{\max}}$ and H_{\max} , T_p and H_{m0} deviate from these ranges, and it does not follow a particular trend (Fig. 2). We obtain one set of data having lesser wave heights (black scatter in Fig. 2) and another one with higher wave heights (blue scatter in Fig. 2). June, July and August are the months with larger wave heights (blue scatter in Fig. 2), and the trend falls between slopes 3.9 and 6.7. It is clear that a few data falls in between the lines having slopes 2.6 and 3.9 and the majority of higher wave heights are in between 3.9 and 6.7. The dashed lines in Fig. 2 represent the three slopes (2.6, 3.9 and 6.7).

Here, we find the relation of $H_{1/10}$ and H_{\max} with $H_{1/3}$ (Fig. 3a and 3b). We observe that $H_{1/10}$ is less spread compared to H_{\max} values. Along the study location, $H_{1/10}$ is approximately equal to 1.24 times the value of $H_{1/3}$ (Fig. 3a), and H_{\max} is approximately 1.65 times the value of $H_{1/3}$ (Fig. 3b), which is consistent with the theoretical values (Longuet-Higgins, 1952). Amrutha and Kumar (2017) reported that H_{\max} is 1.50-1.62 times $H_{1/3}$ for the high waves in the eastern Arabian Sea. For cyclone-generated waves, the average value of the ratio between H_{\max} and $H_{1/3}$ is 1.66 (Kumar et al., 2020).

The energy wave period ($T_{m-1,0}$) is a key parameter in offshore power calculations. It may not be readily available and can be calculated from T_p if it is available (Kamranzad et al., 2013). The energy wave period can be estimated from T_p as $T_{m-1,0} = 0.9 T_p$ for a standard JONSWAP spectrum with a peak enhancement factor of $\gamma = 3.3$ (Contestabile et al., 2015). Here, we try to find whether this relation holds true for the waves in the coastal waters along the eastern Arabian Sea. The variation of the average wave period ($T_{m-1,1}$) with $T_{1/3}$ (Fig. 3c) and the energy wave period with T_p

(Fig. 3d) is derived using the data for 2011. A strong correlation between the $T_{m-1,1}$ and $T_{1/3}$ is clear. For lower values, $T_{1/3}$ approximately matches $T_{m-1,1}$ (Fig. 3c). Kumar and Mandal (2022) investigated the relation between $T_{m-1,1}$ and $T_{1/3}$ at four different locations, including our study area along the eastern Arabian Sea. They affirm that both the wave periods correlate well with a coefficient of 0.88-0.94. The correlation between the $T_{m-1,0}$ and T_p is not as strong. It shows different trends for T_p less than 6 s and greater than 10 s (Fig. 3d). In addition, they are widespread for higher values of T_p . According to Ahn (2021), the energy wave period of the total sea geographically varies from 0.79 to 0.85 times T_p along the US coastal waters. However, along the eastern Arabian Sea, the following relationships are obtained between these characteristic wave periods.

$$T_{m-1,1} = 0.76 T_{1/3} + 1.18 \quad (3)$$

$$T_{m-1,0} = 0.29 T_p + 4.85 \quad (4)$$

3.3 Variations in wave height and period distributions

The probability of exceedance of observed characteristic wave heights ($H_{1/3}$, $H_{1/10}$ and H_{max}) and corresponding wave periods ($T_{1/3}$, $T_{1/10}$ and T_{Hmax}) for the years having more than 95% data is illustrated in Fig. 4. The exceedance probabilities for a given wave height $H_{1/3}$ are presented on a logarithmic scale to show both the average values (slightly below the 50% level) and the values occurring for about 10 hours per year (0.11%, near the lower end of the graph). Large inter-annual variations in the exceedance probability of wave heights are observed in 2012 towards higher wave heights. Kumar and George (2016) indicate that the number of higher wave heights were the least in 2012. Perhaps the eastern Arabian Sea may have experienced some kind of wind or monsoon variability in 2012 compared to other years, both of which can cause large inter-annual variations in the wave heights. The monsoon is a dominant mode of variability in the northern Indian Ocean, which accounts for about 92% of the total variability (Anoop et al., 2015). From 1979 to 2012, the annual mean wind speed along the eastern Arabian Sea shows a statistically significant decreasing trend of $1.5 \text{ cm s}^{-1} \text{ year}^{-1}$ (Shanas and Kumar, 2014). The rest of the years follow a comparable pattern.

The inter-annual variability is not notable for lower wave height and period, and it is remarkable for a H_{max} greater than 4 m (Fig. 4c). The percentage of sea states having a H_{max} greater than 4 m is the highest in 2016 (6.30%) and the lowest in 2012 (3.61%). The other years have more than 5% data with H_{max} greater than 4 m. Even though $H_{1/3}$ in 2012 shows significant variation from the others (Fig. 4a), $T_{1/3}$ does not exhibit any considerable differences (Fig. 4d). Similarly, the $T_{1/3}$ and $T_{1/10}$ of 2014 show significant inter-annual variabilities (Fig. 4d and Fig. 4e, respectively), but

the corresponding wave heights do not. The exceedance probabilities of wave heights in 2014 and 2018 were larger, while that of wave periods are lesser than the rest. There are no considerable inter-annual variations in the probabilities of $T_{H_{\max}}$ (Fig. 4f).

3.4 Short-term statistics of high waves

Here, we focus on the wave and crest height distributions of high waves ($H_{1/3} > 3$ m) to understand the variability of the severe wave field. Data during 2010-2020 has been utilised for further analysis, out of which 2010 has only two data with $H_{1/3} > 3$ m. The number of data with high waves varies each year from a maximum of 415 in 2018 to a minimum of 26 in 2013 (Table 3). The sea state that has the maximum wave height is selected from each year, as well as the calculated ratio of their crest height (H_c) and trough depth (H_t) to the respective wave height (H). These results are shown in Table 3. The mean value of the ratios remains roughly the same every year. The crest height to the corresponding wave height ratio ranges from 0.3 to 0.8, with an annual mean ranging from 0.57 to 0.60. The minimum occurred in 2017 and the maximum occurred in 2013. The crest height of the highest waves in different years varies from 1.06 to 1.62 times the $H_{1/3}$ of the corresponding 30-min data (Table 2). The crest height is 1.55 and 1.63 times the $H_{1/3}$ for the highest waves recorded elsewhere, such as the New Year wave and Andrea wave, largest waves recorded in the North Sea (Bitner-Gregersen et al., 2014).

The wave spectrum for the record having the highest $H_{1/3}$ in different years is examined along with the annual average wave spectrum and the pre-monsoon (Feb-May) average wave spectrum (Fig. 5). It can be seen that the wave spectrum is double-peaked, with low-frequency swells and high-frequency wind-seas during the pre-monsoon period (Figs. 5g to 5l), while during the high wave events, the wave spectrum is single-peaked with extremely high spectral energy (Fig. 5a to 5f). In all years, during the high wave events, the wave spectrum is narrow, and the spectral peak lies predominantly in the swell region (mostly between 0.075 and 0.095 Hz), indicating the presence of high energy swells reaching the measurement location. The spectral narrowness parameter is low (0.45-0.50) for all the records having the highest $H_{1/3}$ in a year, compared to that of the pre-monsoon (0.58-0.64) and annual average wave spectrum (0.55-0.59). When combined sea states consisting of long-period and short-period waves are present, the spectral narrowness parameters have a high value, which indicates a broad-banded spectrum. Most of the time, the spectral energy of the wave fields of the eastern Arabian Sea is concentrated on a wide range of frequencies and directions i.e., broad-banded sea state. Variation in the spectral width parameter is similar to that of the spectral narrowness parameter (Fig. 6a). The wave spectrum for the highest waves has a Q_p ranging from 2.0 to 4.1 in different years, while that for the annual average wave spectrum is 1.3-2.3 (Fig. 6). For the

narrow-band spectrum, the spectral peakedness parameter is relatively higher than those for the broad-band wave spectrum (Fig. 6b).

Kurtosis, the fourth order moment of the probability density function of the sea surface elevation, gives a measure of the importance of the tails of the distribution (i.e., information on the percentage of extremes in the record). The kurtosis of the surface elevation is found to increase with the abnormality ratio ($H_{1/3}/H_{max}$) (Fig. 6c), while the skewness (the degree of vertical asymmetry of the surface elevation) does not show a strong correlation with the abnormality ratio (Fig. 6d). Mori et al. (2011) observed that the role of the skewness in the wave height distribution is less important than kurtosis. The skewness comes usually as a result of second-order corrections (bound modes) and is weakly affected by the dynamics of free waves (Onorato et al. 2005). Kurtosis varies for swell and wind-sea dominated sea states with smaller values in swell-dominated conditions than for wind-sea-dominated conditions (Petrova and Guedes Soares, 2008). The directional width or the spread parameter is low ($12.2-17.7^\circ$) for all the records having highest $H_{1/3}$ in a year, compared to that of the pre-monsoon ($31.2-35.2^\circ$) and annual average wave spectrum ($12.5-30.6^\circ$) (Fig. 5). Kumar and Anoop (2013) observed that the directional spreading of wind-sea dominated wave spectrum is less ($\sim 18^\circ$) than that of the swell dominated spectrum ($\sim 24^\circ$). The nonlinear effects of surface waves increase as the waves move from deeper to shallow waters and start to feel the seabed, and this may have an effect on the presented results since the data used in the study are from a water depth of 15 m.

The measured distributions of individual wave heights within sea states with significant wave heights exceeding 3 m are compared with the wave height distributions. Here, wave heights are normalized by m_0 (moment of zero-order). Fig. 7 depicts the exceedance probability predicted by different models and that of observed data (dashed line) for the sea states having maximum $H_{1/3}$ in a year from 2011 to 2020. Since there are only two data available in 2010, we exclude them. As can be seen, the observed data generally agrees well with the Rayleigh distribution at higher normalised wave heights for most of the years. The Rayleigh distribution seems to be a little over-predictive. Earlier studies support the conclusion that the Rayleigh distribution overpredicts the heights of the larger waves in a record (Casas-Prat and Holthuijsen, 2010). Even though the Rayleigh model falls into the deep-water model category, it is widely applied in all water depths. It also agrees with the Forristall distribution in 2014, 2015, 2016 and 2018. The Forristall distribution has been widely adopted in both deep and intermediate water depths. For lesser normalized wave heights, the observed data does not coincide with any of these models except for the Longuet-Higgins distribution at some points. In short, for estimating the extreme wave heights along the study area,

the Rayleigh distribution will be appropriate, followed by the Forristall distribution. The study by Longuet-Higgins (1952) pointed out that the wave heights will be Rayleigh distributed if the wave spectrum becomes extremely narrow. The probability of wave heights to exceed 3 m is less than 40% and that of 4 m is less than 20% only. Similarly, the distributions for crest heights have also been estimated, and it is found that the normalized crest heights (normalized by $H_{1/3}$) are Rayleigh distributed (Fig. 8). Fig. 8 indicates that the Rayleigh distribution exactly obeys the measured values towards higher crest heights, and it falls inside the 95% confidence interval. Meanwhile, none of the other models agree with the observed data well. Further, in every year, the probability of crest heights to exceed 0.5 m is below 20%. Fernandez et al. (2016) observed that for shallower water depth, departure from second order distribution in the unidirectional sea states vanishes and crest heights fit the Forristall distribution. The data with $H_{1/3}$ more than 3 m used in the study falls in intermediate water depth with d/L values ranging from 0.09 to 0.15. Fig. 9 shows the scatter plot of bias with $H_{1/3}$ for various distributions. The symbol size is proportional to the spectral narrowness parameter and the colour is as per the spectral width parameter. The bias between the data and Rayleigh distribution is less for narrow banded spectra. The wave field obeys the Gaussian statistics when it is narrow banded, and hence it follows the Rayleigh distribution.

Although the Rayleigh model best matches the observed data for the extreme sea state, the Van Vledder distribution exhibits less bias when the entire set of data is taken into account (Fig. 10). Shoaling alters the shape of the distribution as the waves get closer to the coast. Van Vledder (1991) distribution is thus proposed to take the shallow-water effects into account. The bias between distribution models and the observed data for all the sea states with significant wave height more than 3 m is shown in Fig. 10. It can be seen that the Rayleigh, Forristall and Van Vledder distributions have the least error. The Rayleigh distribution is biased 0-0.05 higher than the observed data except at one point where it is biased 0.007 lower than the observed data. The two models with the highest error are Longuet-Higgins and Klopman, as the former underestimates the observed data while the latter overestimates it. Klopman (1996) distribution is mainly for very shallow-waters, whereas all the waves used in the study are intermediate or deep-water waves.

Similar studies have been carried out in many ocean basins. James and Panchang (2022) investigated the short-term statistics of wave conditions in the coastal waters of UK using more than 40,000 half-hour-long sea states. According to them, the relative wave height is an important factor in choosing the wave height distribution with the least error for a given sea state. For the sea states having low relative wave heights, the Naess model is the most accurate in describing the tail of the wave height distribution and the Van Vledder model for high relative wave heights (James and

Panchang, 2022). The data from the central and southern North Sea have been utilised by Karpadakis et al. (2020), who examined the accuracy of nine wave height distribution models under a range of conditions. They showed that no single model accurately describes the measured wave heights across different conditions. However, the Boccotti distribution gives better approximations for low relative wave heights, and as it increases, the Van Vledder, Mendez and Battjes-Groenendijk models fit well.

Tayfun and Fedele (2007) conducted studies using wave heights measured at a deep-water platform in the North Sea and found that they also agree well with the Boccotti distribution. Kvingedal et al. (2018) utilized data from the northern North Sea at a water depth of around 190 m and found that the Forristall distribution has good accuracy while the Rayleigh distribution behaves as a conservative upper bound. Casas-Prat and Holthuijsen (2010) examined the short-term statistics of 10 million deep water waves in the Mediterranean Sea off the coast of Spain. They could find that normalized crest heights and trough depths are Rayleigh distributed, but the normalized wave heights are not. There, the wave heights are well predicted by Rayleigh-like distributions obtained from linear theories and by empirical Weibull distributions. However, in the eastern Arabian Sea off Karwar, the Rayleigh distribution has the greatest accuracy in predicting the most severe sea state. This result is consistent with the findings of Dattatri et al. (1979), who used the wave height data from the Mangalore coast, which is also along the eastern part of the Arabian Sea.

4. Conclusions

In this study, the short-term statistics of wave conditions in the nearshore waters of Karwar are investigated using 172704 half-hour-long records. The highest individual waves reached 8.3 m. The mean monthly averaged d/L value is 0.62, indicating that all the measured waves are in intermediate and deep waters, and the results also show that the waves with a significant wave height ($H_{1/3}$) of more than 3 m are in intermediate water. For estimating $H_{1/10}$ and H_{max} , the significant wave height ($H_{1/3}$) is utilized. $H_{1/10}$ is 1.24 times $H_{1/3}$ and the maximum wave height, H_{max} , is 1.65 times $H_{1/3}$. There is considerable inter-annual variability in the exceedance probabilities of wave heights in 2012, and there is no such significant variability for T_{Hmax} . The energy wave period along the study area cannot be correlated to the spectral peak period as indicated by earlier studies (Kamranzad et al., 2013; Contestabile et al., 2015), and it shows different trends for lower and higher values of the peak period. Moreover, a best-fit slope between the characteristic wave period and the corresponding wave height could not be obtained, as in ISSC (1979). Instead, we define a range of slopes to understand the relation during southwest monsoon months (June-July-August), when there are higher wave heights.

The analysed wave spectrum for the annual average wave heights, the pre-monsoon average wave heights and the record with the highest $H_{1/3}$ reveal the presence of low-frequency swells and high-frequency wind-seas during the pre-monsoon period. During high wave events, the spectrum is narrow and single-peaked, with the peak lying in the swell region. The exceedance probability of normalized wave heights of high waves ($H_{1/3} > 3$ m) agrees with the Rayleigh, Forristall and Van Vledder distributions. However, for the most extreme sea states, only the Rayleigh distribution displayed the least error. Similarly, crest heights of the extreme sea state also follow the Rayleigh distribution. Besides, the crest height of the largest wave in different years was 0.57 to 0.60 times the wave height.

Author Contributions:

Anusree A - data analysis and original draft

Sanil Kumar -data analysis and editing

Funding: This research received no external funding.

Acknowledgements

The authors acknowledge the ESSO-Indian National Centre for Ocean Information Services (INCOIS), Ministry of Earth Sciences for funding the wave measurements at Karwar. We thank TM. Balakrishnan Nair, Head OSISG, Arun Nherakkol, Scientist, INCOIS, Hyderabad, Jai Singh, Technical Officer, CSIR-NIO for help during data collection. We thank Dr. JL Rathod, Department of Marine Biology, Karnataka University PG Centre, Karwar for providing the logistics required for wave data collection. The authors thank both the reviewers for the comments and suggestions, which improved the content of the paper. This publication is an NIO contribution ---

Conflicts of Interest: The authors declare no conflicts of interest.

References

- Ahn, S., 2021. Modeling mean relation between peak period and energy period of Ocean Surface Wave Systems. *Ocean Engineering* 228, 108937. doi:10.1016/j.oceaneng.2021.108937.
- Amrutha, M.M., Kumar, V.S., 2015. Short-term statistics of waves measured off Ratnagiri, eastern Arabian Sea. *Applied Ocean Research* 53, 218–227. doi:10.1016/j.apor.2015.09.009.
- Amrutha, M.M., Sanil Kumar, V., 2017. Characteristics of high monsoon wind-waves observed at multiple stations in the eastern Arabian Sea. *Ocean Science Discussions*, 1–30. <https://doi.org/10.5194/os-2017-84>.

- Anoop, T.R., Kumar, V.S., Shanas, P.R., Johnson, G., 2015. Surface wave climatology and its variability in the North Indian Ocean based on era-interim reanalysis. *Journal of Atmospheric and Oceanic Technology* 32, 1372–1385. doi:10.1175/jtech-d-14-00212.1
- Battjes, J. A., 1970. Long-term wave height distributions at seven stations around the British Isles. Internal Rep, Nat Inst Oceanogr Wormley No: A 44.
- Bitner-Gregersen, E.M., Fernandez, L., Lefèvre, J.M., Monbaliu, J., Toffoli, A., 2014. The North Sea andrea storm and numerical simulations. *Natural Hazards and Earth System Sciences* 14, 1407–1415. doi:10.5194/nhess-14-1407-2014.
- Casas-Prat, M., Holthuijsen, L.H., 2010. Short-term statistics of waves observed in Deep Water. *Journal of Geophysical Research* 115. doi:10.1029/2009jc005742.
- Contestabile, P., Ferrante, V., Vicinanza, D., 2015. Wave Energy Resource along the coast of Santa Catarina (Brazil). *Energies* 8, 14219–14243. doi:10.3390/en81212423.
- Datawell., 2009. Datawell Waverider Reference Manual, Datawell BV oceanographic instruments, The Netherlands, p 123.
- Dattatri, J., Raman, H., Shankar, N.J., 1979. Height and period distributions for waves off Mangalore Harbour-West Coast. *Journal of Geophysical Research* 84, 3767. doi:10.1029/jc084ic07p03767.
- Dora, G.U., Kumar, V.S., 2015. Sea state observation in island-sheltered nearshore zone based on in situ intermediate-water wave measurements and NCEP/CFSR Wind Data. *Ocean Dynamics* 65, 647–663. doi:10.1007/s10236-015-0822-1.
- Fernandez, L., Onorato, M., Monbaliu, J., Toffoli, A., 2016. Occurrence of Extreme Waves in Finite Water Depth. In: Pelinovsky, E., Kharif, C. (eds) *Extreme Ocean Waves*. Springer, Cham. https://doi.org/10.1007/978-3-319-21575-4_3.
- Forristall, G.Z., 1978. On the statistical distribution of wave heights in a storm. *Journal of Geophysical Research* 83, 2353. doi:10.1029/jc083ic05p02353
- Goda, Y., 2010. *Random seas and design of maritime structures*. Advanced Series on Ocean Engineering. World Scientific, 708 pp.
- Goda, Y., 1970. Numerical experiments on wave statistics with spectral simulation, Report Port and Harbour Research Institute, Japan, 9, 3–57.
- Guedes Soares, C., 2003. Probabilistics Models of waves in the coastal zone. In: Lakhan, V.C. (Ed.), *Advanced in Coastal Modelling*. Elsevier.
- ISSC, 1979: Report of Committee I.1: (Environmental conditions). 7th International Ship Structures Congress, Paris.
- James, J.P., Panchang, V., 2022. Investigation of wave height distributions and characteristic wave periods in coastal environments. *Journal of Geophysical Research: Oceans* 127. doi:10.1029/2021jc018144.
- Kamranzad, B., Etemad-shahidi, A., Chegini, V., 2013. Assessment of wave energy variation in the Persian Gulf. *Ocean Engineering* 70, 72–80. doi:10.1016/j.oceaneng.2013.05.027.

- Karmpadakis, I., Swan, C., Christou, M., 2020. Assessment of wave height distributions using an extensive field database. *Coastal Engineering* 157, 103630. doi:10.1016/j.coastaleng.2019.103630.
- Kinsman, B., 1965. *Wind waves: their generation and propagation on the ocean surface*. Prentice-Hall. 676 pp.
- Klopman, G., 1996. *Extreme wave heights in shallow water*. Delft Hydraulics Report H2486WL
- Kuik, A. J., Vledder, G., and Holthuijsen, L. H., 1998. A method for the routine analysis of pitch and roll buoy wave data. *J. Phys. Oceanogr.*, 18, 1020-1034.
- Kumar, V.S., Anoop, T.R., 2013. Directionality and spread of shallow water waves along eastern Arabian Sea, *Annales Geophysicae*, 31, 1817–1827, doi:10.5194/angeo-31-1817-2013
- Kumar, V.S., George, J., 2016. Influence of Indian summer monsoon variability on the surface waves in the coastal regions of eastern Arabian Sea. *Annales Geophysicae* 34, 871–885. doi:10.5194/angeo-34-871-2016.
- Kumar, V.S., Harikrishnan, S., Mandal, S., 2020. Wave crest height distribution during the tropical cyclone period. *Ocean Engineering* 197, 106899. doi:10.1016/j.oceaneng.2019.106899.
- Kumar, V.S., Mandal, S., 2022. Characteristics of individual surface waves measured by moored buoys in the coastal waters of the eastern Arabian Sea. *Ocean Engineering* 248, 110861. doi:10.1016/j.oceaneng.2022.110861.
- Kvingedal, B., Bruslerud, K., Nygaard, E., 2018. Individual wave height and wave crest distributions based on field measurements from the northern North Sea. *Ocean Dynamics* 68, 1727–1738. doi:10.1007/s10236-018-1216-y.
- Longuet-Higgins, M. S., 1952. On the statistical distribution of the heights of Sea waves. *Journal of Marine Research*, 11(3), 245– 266.
- Longuet-Higgins, M. S., 1975. On the joint distribution of the periods and amplitudes of sea waves. *J. Geophys. Res.* 80(18), 2688-2694.
- Mathisen, J., Bitner-Gregersen, E., 1990. Joint distributions for significant wave height and wave zero-up-crossing period. *Applied Ocean Research* 12, 93–103. doi:10.1016/s0141-1187(05)80033-1.
- Mori, N., Janssen, P. A. E. M., 2006. Freak wave prediction from directional spectra. *Proc. 30th Int. Conf. Coastal Engineering 2006*, J. M. Smith, Ed., World Scientific, 714–725.
- Mori, N., Onorato, M., Janssen, P. A. E. M., 2011. On the Estimation of the Kurtosis in Directional Sea States for Freak Wave Forecasting. *J. Phys. Oceanogr.* 41, 1484–1497, <https://doi.org/10.1175/2011JPO4542.1>.
- Nair, M.A., Amrutha, M.M., Kumar, V.S., 2022. Spectral wave characteristics in the coastal waters of the central west coast of India during tropical cyclone Kyarr, *Ocean Dynamics*, 72:151–168, <https://doi.org/10.1007/s10236-022-01496-x>
- Nayak, S., Panchang, V., 2015. A note on short-term wave height statistics. *Aquatic Procedia* 4, 274–280. doi:10.1016/j.aqpro.2015.02.037.

- Petrova, P., Guedes Soares, C., 2008. Maximum wave crest and height statistics of irregular and abnormal waves in an offshore basin. *Appl Ocean Res* 30:144–152. <https://doi.org/10.1016/j.apor.2008.08.004>.
- Ochi, M.K., 1998. *Ocean Waves, the Stochastic Approach*. Cambridge Univ. Press, 319 pp.
- Onorato, M., Osborne, A., Serio, M., Bertone, S., 2005. On deviations from Gaussian statistics for surface gravity waves. *Rogue Waves: Proc. 'Aha Huliko'a Hawaiian Winter Workshop*, Honolulu, HI, University of Hawaii at Manoa, 79–83.
- Orimoloye, S., Harshinie K., Reeve, D.E., 2019. Effects of Swell on Wave Height Distribution of Energy-Conserved Bimodal Seas. *Journal of Marine Science and Engineering* 7, no. 3: 79. <https://doi.org/10.3390/jmse7030079>.
- Schott, F.A., McCreary, J.P., 2001. The monsoon circulation of the Indian Ocean. *Progress in Oceanography* 51, 1–123. doi:10.1016/s0079-6611(01)00083-0.
- Shanas, P.R., Kumar, V.S., 2014. Temporal variations in the wind and wave climate at a location in the eastern Arabian Sea based on era-interim reanalysis data. *Natural Hazards and Earth System Sciences* 14, 1371–1381. doi:10.5194/nhess-14-1371-2014.
- Stansell, P., 2004. Distributions of freak wave heights measured in the North Sea. *Appl. Ocean Res.*, 26, 35–48, doi:10.1016/j.apor.2004.01.004.
- Sverdrup, H. U., Munk, W. H. (1947). *Wind, sea and swell: Theory of relations for forecasting* (No. 303). Hydrographic Office. <https://doi.org/10.5962/bhl.title.38751>.
- Tayfun, M.A., Fedele, F., 2007. Wave-height distributions and nonlinear effects. *Ocean Engineering* 34, 1631–1649. doi:10.1016/j.oceaneng.2006.11.006
- Tucker, M.J., 1991. *Waves in ocean engineering: measurement, analysis, interpretation*. Ellis Horwood, Chichester, UK. 431 pp.
- van Vledder, G. P., 1991. Modification of the Glukhovskiy distribution. Technical report, Delft Hydraulics Report H, 1203.
- WMO, 1998. *Guide to Wave Analysis and Forecasting*, WMO No.-702, World Meteorological Organization – Geneva – Switzerland.

Appendix-1: Wave height distribution models examined in the study

1. Rayleigh Distribution

$$Q(H) = \exp\left(-\left(\frac{H}{a}\right)^2\right)$$

Where $a = H_{rms}$

2. Spectral Rayleigh Distribution

$$Q(H) = \exp\left(-\left(\frac{H}{a}\right)^2\right)$$

Where $a = \sqrt{8m_0}$

3. Forristall Distribution

$$Q(H) = \exp\left(-\frac{1}{\beta}\left(\frac{H}{\sqrt{m_0}}\right)^\alpha\right)$$

Where $\alpha = 2.126$ and $\beta = 8.42$

4. Longuet-Higgins Distribution

$$Q(H) = \exp\left(-\frac{1}{1-0.734\nu^2}\left(\frac{H}{\sqrt{8m_0}}\right)^2\right)$$

Where ν is the spectral bandwidth

5. Klopman Distribution

$$Q(H) = \exp\left(-A\left(\frac{H}{H_{rms}}\right)^K\right)$$

Where $A = \frac{2}{1-\frac{\beta H_{rms}}{D}}$, $A = \left(\Gamma\left(\frac{2}{K} + 1\right)\right)^{\frac{K}{2}}$ and $\beta = 0.7$

6. Van Vledder Distribution

$$Q(H) = \exp\left(-A\left(\frac{H}{H_m}\right)^K\right)$$

Where $K = \frac{2}{1-\frac{H_m}{D}}$, $A = \Gamma\left(\frac{1}{K} + 1\right)^K$ and Γ is the gamma function.

Table 1. Percentage of waves in different groups based on height and number of waves. The years having maximum number of data (greater than 95%) has shown in bold.

Year	Data (%)	Annual average $H_{1/3}$ (m)	Annual average H_{max} (m)	Average height	$H_{1/3} \leq 1.5m$	$1.5m < H_{1/3} < 3m$	$H_{1/3} \geq 3m$	Number of waves	d/L
2010	70.58	0.63	1.08		95.14	4.84	0.02		
2011	99.98	1.02	1.73	0.65	74.16	24.93	0.91	5534980	0.63
2012	98.61	1.00	1.73	0.65	74.55	25.34	0.11	5460034	0.61
2013	82.94	0.81	1.39		94.30	5.51	0.19		
2014	98.65	0.97	1.65	0.62	80.81	17.42	1.76	5464264	0.63
2015	84.32	1.00	1.71		80.39	17.84	1.77		
2016	96.20	1.05	1.78	0.69	75.83	22.09	2.08	5395125	0.62
2017	99.46	1.04	1.76	0.66	74.99	23.46	1.54	5497168	0.61
2018	95.21	1.00	1.69	0.62	79.08	18.44	2.49	5491602	0.67
2019	76.44	0.78	1.34		93.90	4.81	1.29		
2020	82.61	1.16	1.95		71.91	25.74	2.35		

Table 2. Characteristics of the wave with maximum height in different years.

Year	Month	day	hour	H_{\max} (m)	$T_{H_{\max}}$ (s)	H_c (m)	H_t (m)	$H_{1/3}$ (s)	length (m)	steepness
2010	6	15	19	4.8	12.0	3.3	1.5	3.1	135	0.0354
2011	9	3	07	6.8	10.8	3.8	2.9	3.3	120	0.0564
2012	7	22	00	6.2	9.9	4.2	2.0	2.6	108	0.0571
2013	6	11	13	7.2	10.3	4.4	2.8	3.0	113	0.0633
2014	6	10	04	7.4	9.2	4.7	2.7	3.4	98	0.0751
2015	6	21	14	7.9	10.6	5.1	2.8	4.3	117	0.0673
2016	6	30	02	8.1	10.1	5.0	3.1	3.7	110	0.0736
2017	7	20	05	7.6	9.0	4.8	2.8	3.7	96	0.0797
2018	7	16	17	7.9	10.8	5.5	2.4	3.7	120	0.0661
2019	10	25	03	8.3	10.2	4.8	3.5	4.1	112	0.0743
2020	8	5	07	8.3	12.3	5.5	2.8	4.1	139	0.0596

Table 3 Range and mean values of the ratios for sea states with significant wave height more than 3 m in a year. H_c , H_t and H are the crest height, trough depth and maximum wave height respectively.

Year	H_c/H		H_t/H		Number of records
	Range	Mean	Range	Mean	
2010	0.68-0.70	0.69	0.30-0.32	0.31	2
2011	0.36-0.72	0.58	0.28-0.64	0.42	154
2012	0.45-0.66	0.58	0.34-0.55	0.42	18
2013	0.43-0.69	0.60	0.31-0.57	0.40	26
2014	0.40-0.75	0.59	0.25-0.60	0.41	297
2015	0.42-0.76	0.59	0.24-0.59	0.41	262
2016	0.42-0.73	0.58	0.27-0.58	0.42	351
2017	0.34-0.73	0.57	0.27-0.66	0.43	256
2018	0.36-0.77	0.58	0.23-0.64	0.42	415
2019	0.39-0.71	0.58	0.29-0.61	0.42	173
2020	0.32-0.75	0.58	0.25-0.68	0.42	338

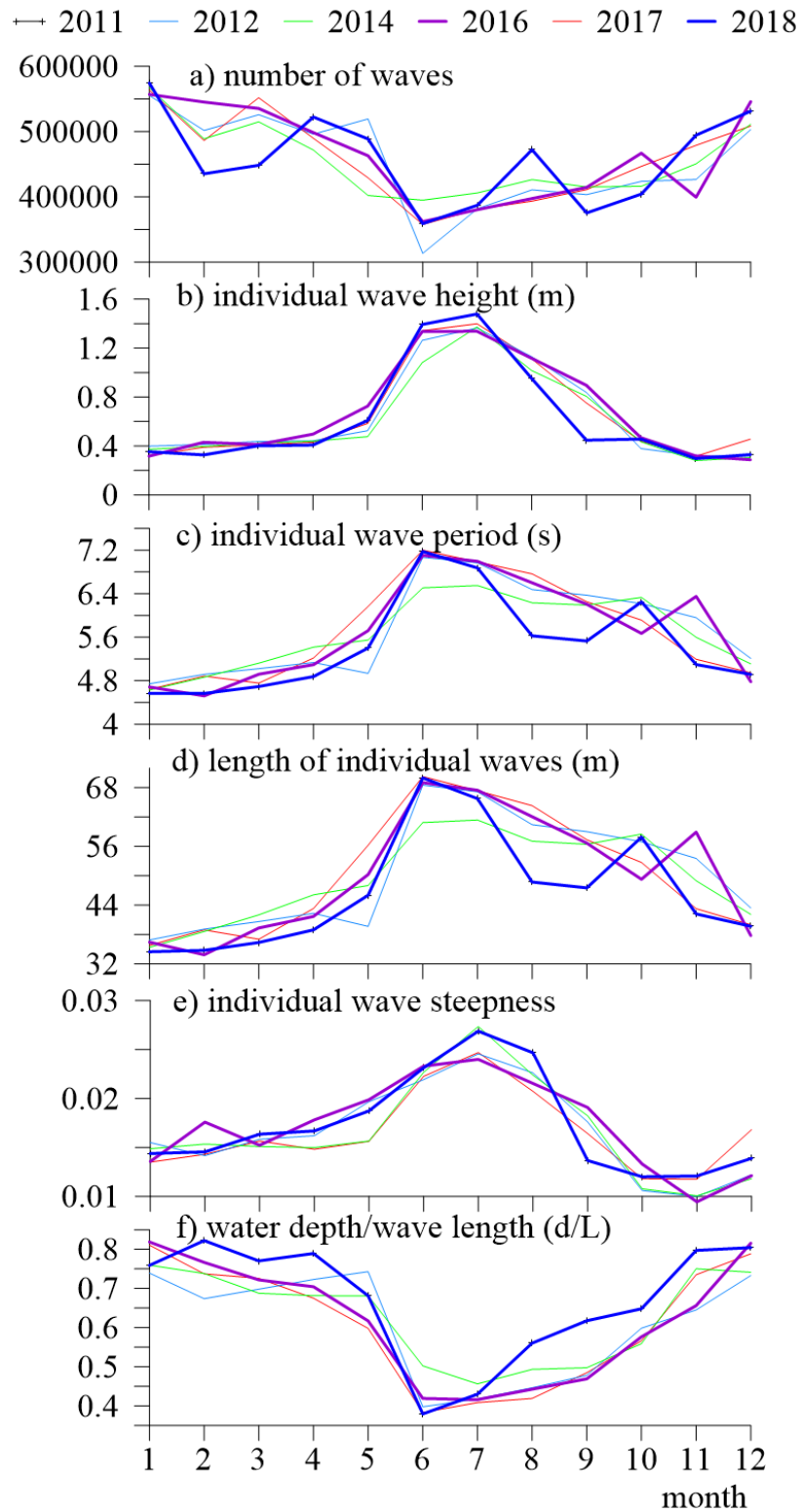


Fig. 1. Plots of a) total number of waves measured in different months, b) monthly mean of individual wave height, c) monthly mean of individual wave period, d) monthly mean of wave length, e) monthly mean of individual wave steepness and f) ratio of water depth and wave length in years 2011, 2012, 2014, 2016, 2017 and 2018

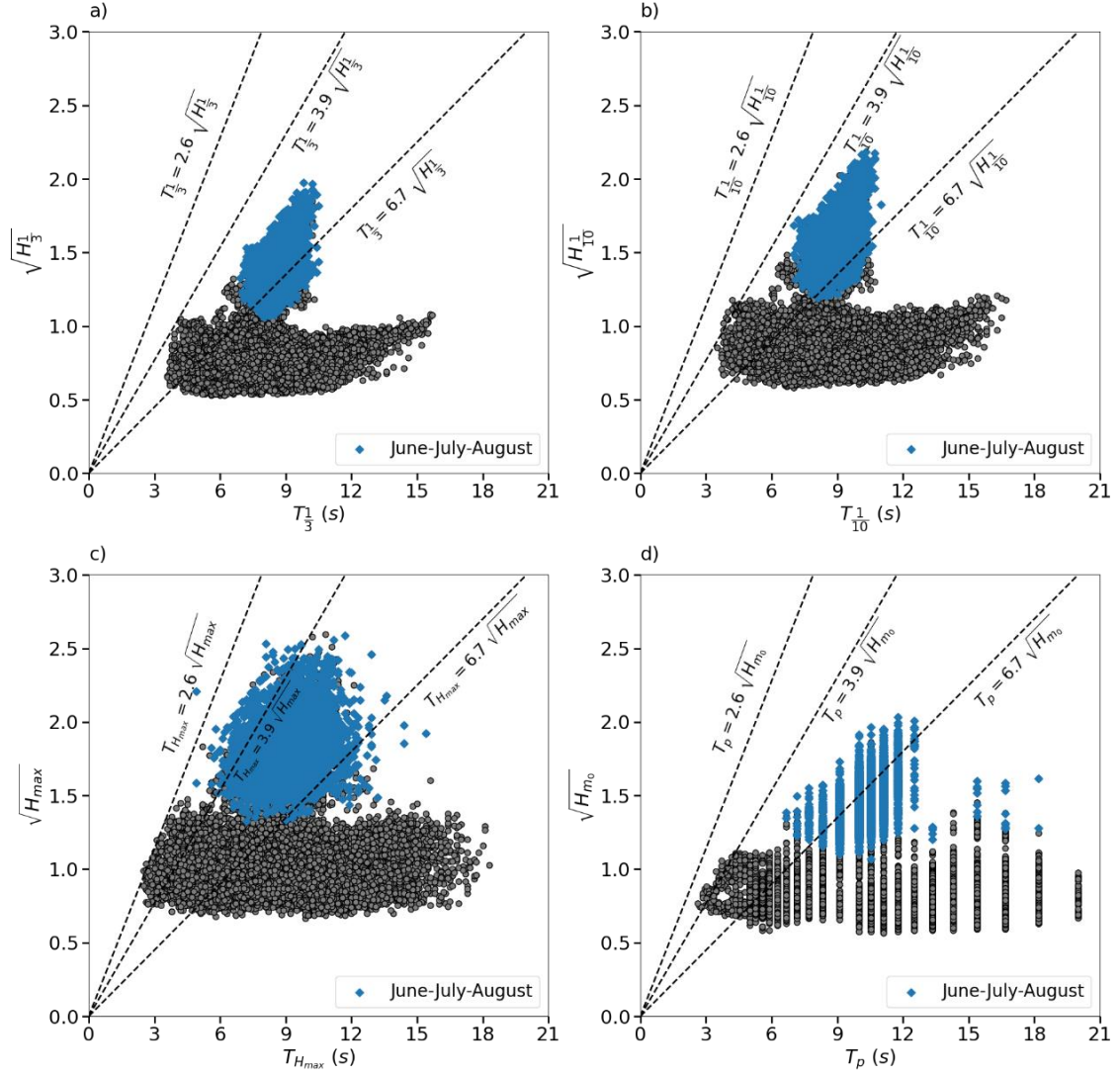


Fig. 2. Scatter plot between a) $T_{1/3}$ and $\sqrt{H_{1/3}}$, b) $T_{1/10}$ and $\sqrt{H_{1/10}}$, c) T_{Hmax} and $\sqrt{H_{max}}$ and d) T_p and $\sqrt{H_{m0}}$ during 2011. Heights and periods are in metres and seconds respectively. The dashed lines represent three different slopes (2.6, 3.9 and 6.7). Blue and black colour indicates data during southwest monsoon (June to August) and the remaining data respectively

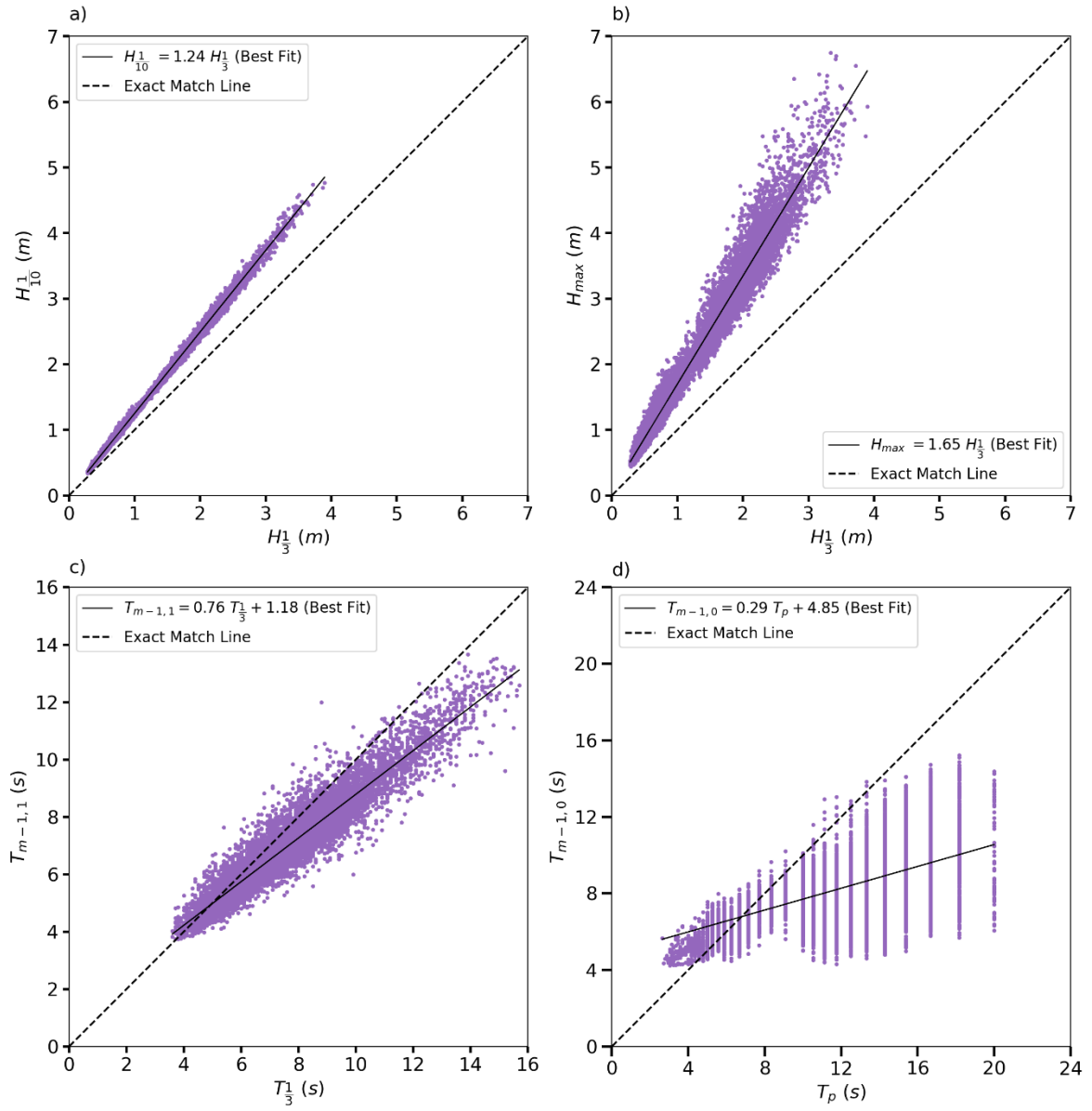


Fig. 3. Plots showing the relation between a) $H_{1/3}$ and $H_{1/10}$, b) $H_{1/3}$ and H_{max} , c) $T_{m-1,1}$ and $T_{1/3}$ and d) $T_{m-1,0}$ and T_p calculated for 2011

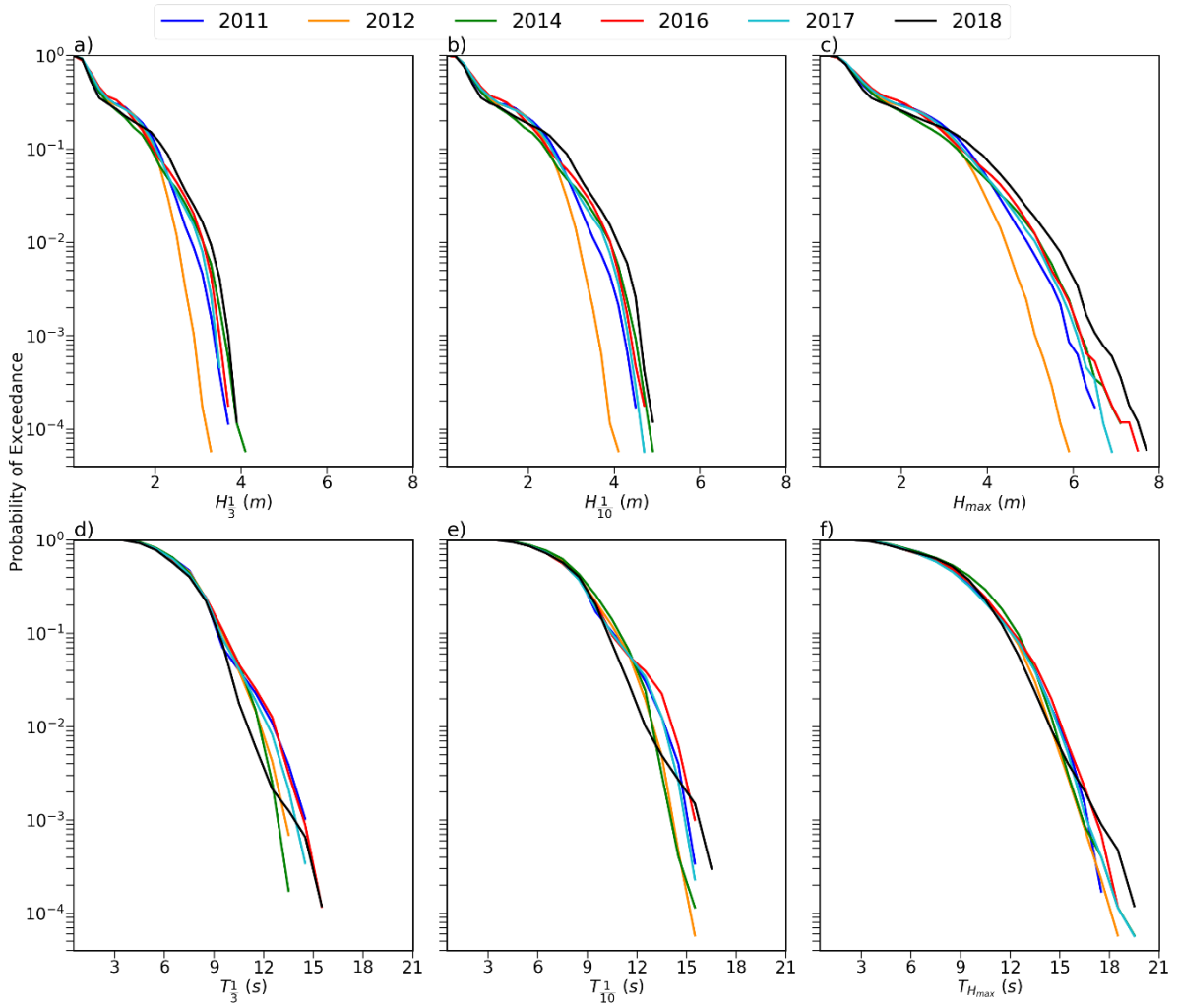


Fig. 4. Probability of exceedance of wave heights a) $H_{1/3}$, b) $H_{1/10}$ and c) H_{max} and wave periods d) $T_{1/3}$, e) $T_{1/10}$ and f) $T_{H_{max}}$ for the years having the maximum number of data. Probability is in logarithmic scale.

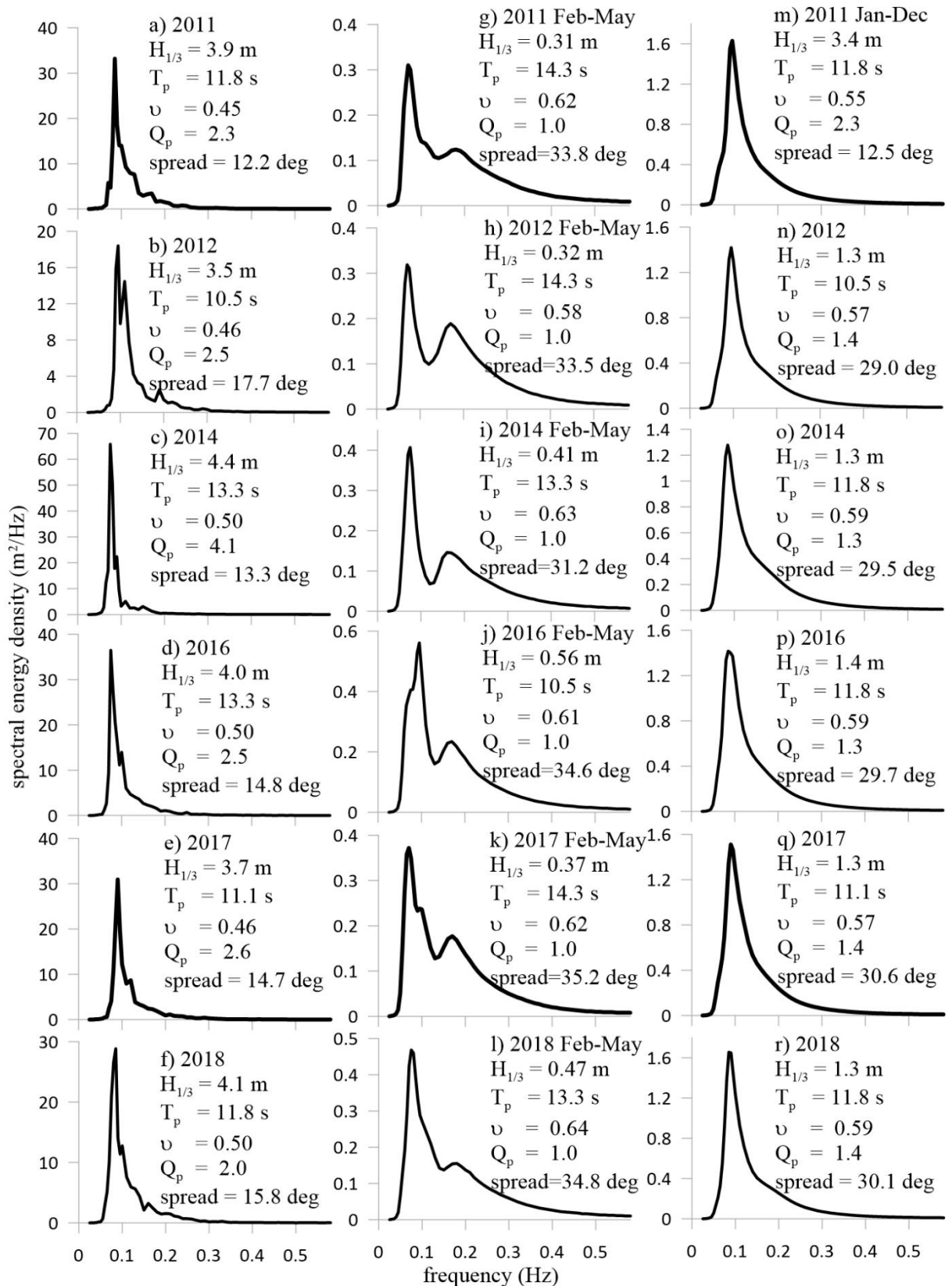


Fig. 5. Plots of wave spectra; a to f) are for records having maximum significant wave height in a year, g to l) are for seasonal average for pre-monsoon (Feb-May) and m to r) are for the annual average for the corresponding year

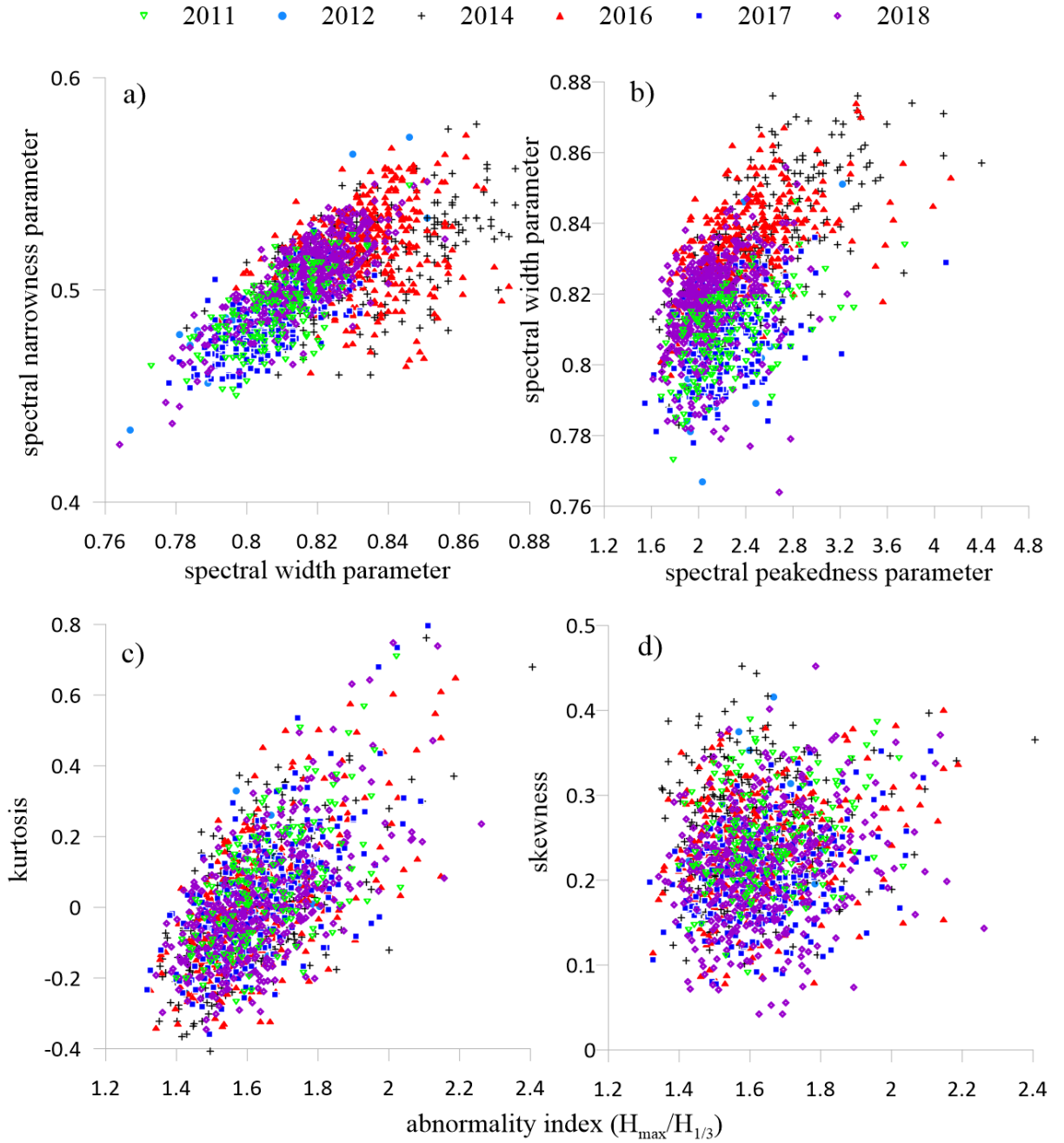


Fig. 6. Scatter plots between a) spectral narrowness parameter and spectral width parameter, b) spectral width parameter and spectral peakedness parameter, c) kurtosis and abnormality index and d) skewness and abnormality index

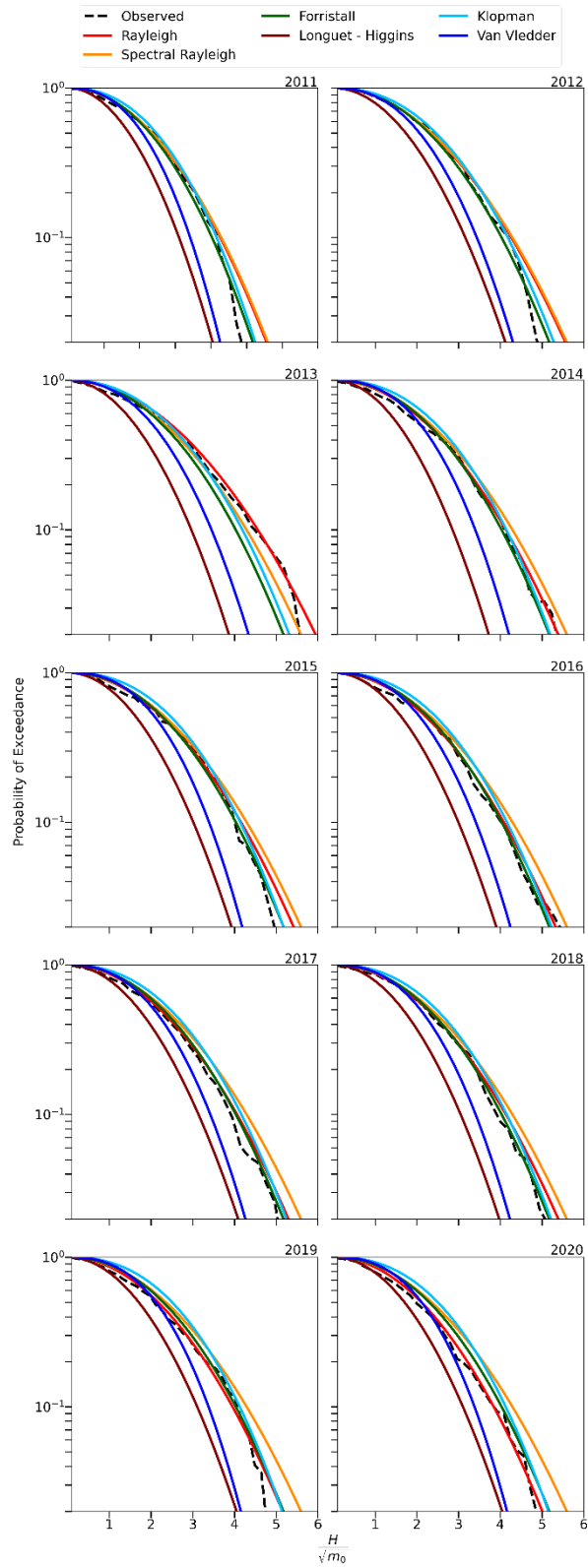


Fig. 7. The probability of exceedance of observed and model wave height data for the sea states having maximum $H_{1/3}$ in different years from 2011 to 2020. H is the individual wave height, which is normalized by m_0

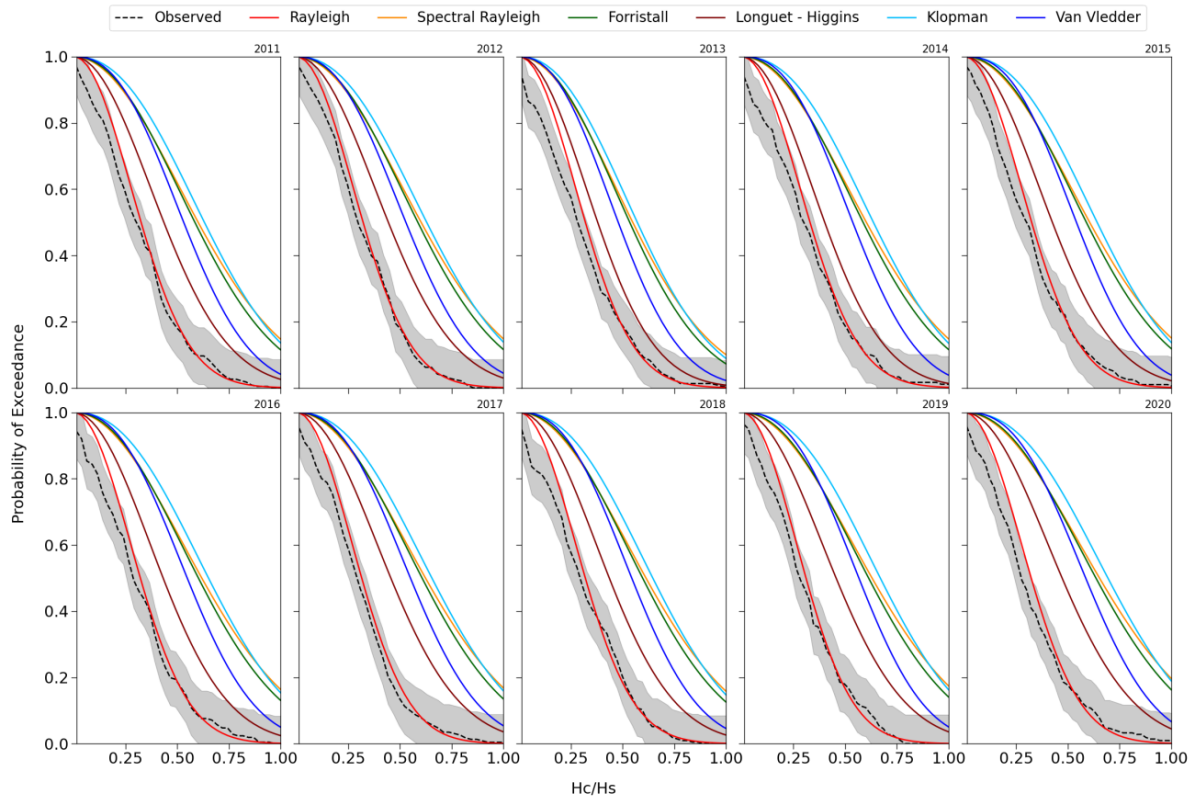


Fig. 8. For the 30-minute-long sea states with maximum $H_{1/3}$, the probability of exceedance of observed and model crest height data is displayed for each year from 2011 to 2020. Crest height is normalized by significant wave height (H_s). Shading represents the 95% confidence interval of the observed crest height distribution

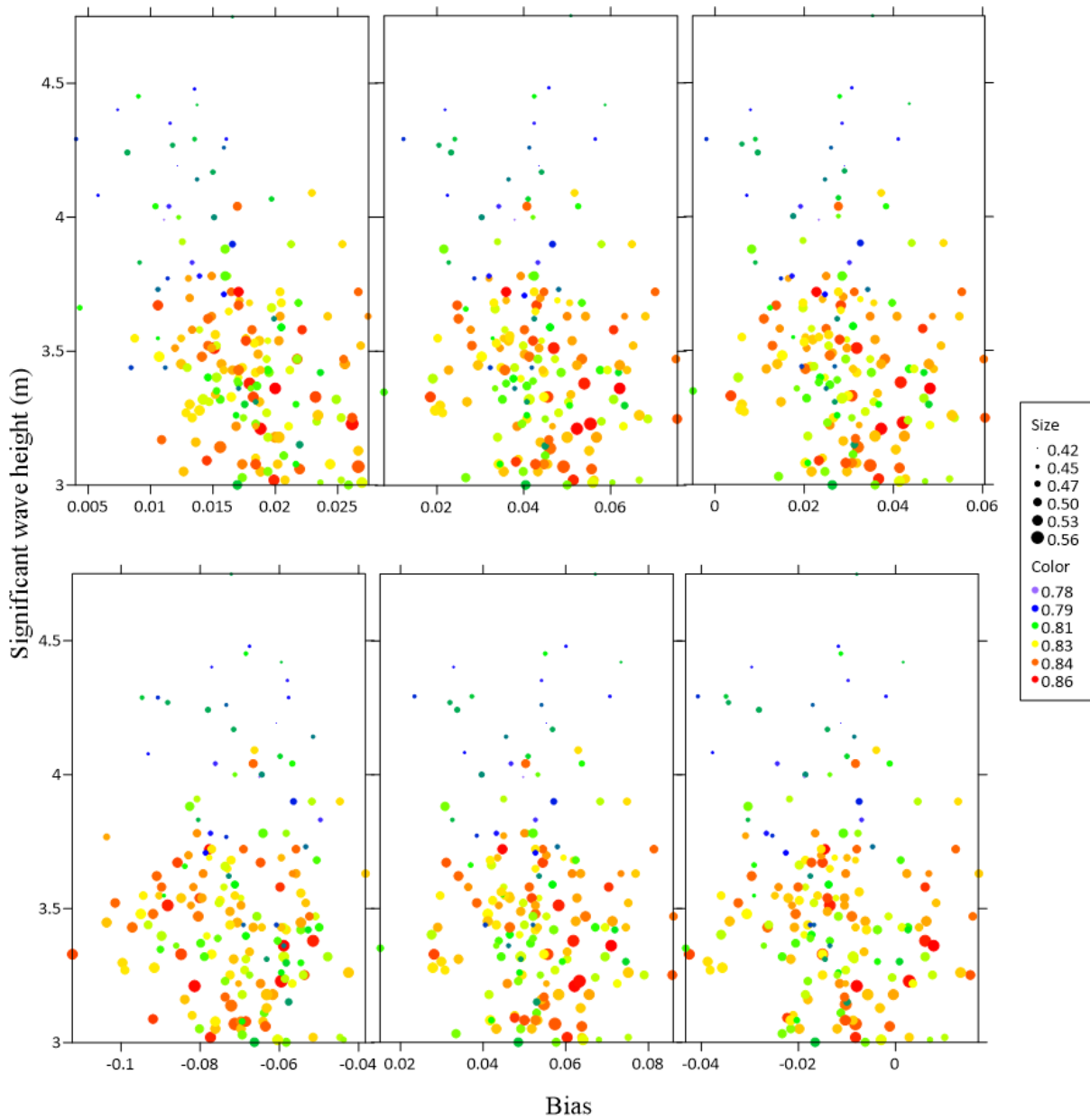


Fig. 9. Scatter plots of bias between observed data and the distribution models calculated for each 30-minute record with significant wave height ($H_{1/3}$) greater than or equal 3 m. The symbol size is proportional to the spectral narrowness parameter and the colour is as per the spectral width parameter



Fig. 10. Bias between observed wave height data and the distribution models calculated for each 30-minute record with significant wave height ($H_{1/3}$) greater than or equal to 3 m. Each plot represents various years from 2011 to 2020.